J Appl Electrochem (2008) 38:1665–1670
DOI 10.1007/s10800-008-9614-3

ORIGINAL PAPER

Ethanol electrooxidation on platinum particles dispersed on poly(neutral red) film

Xinxian Zhong · Jinhua Chen · Xiaohua Zhang

Received: 5 December 2007 / Accepted: 27 May 2008 / Published online: 10 June 2008

Abstract The conductive polymer poly(neutral red) polymerized on a graphite electrode (PNR/graphite) as a support material was used for catalytic oxidation of ethanol in acidic solution and investigated by electrochemical methods. Pt particles loaded on the surface of PNR/graphite electrode exhibited higher electrocatalytic activity for ethanol oxidation in comparison with Pt particles supported directly on graphite. With the equivalent loading mass of Pt catalyst, the special activity (S_A) at peak a of the Pt/PNR/graphite electrode polymerized for 10 cycles in 5×10^{-4} M NR + 0.5 M H_2SO_4 solution is 3,478 A C^{-1} and about 2.20 times higher than that of the Pt/graphite electrode (1,582 A C^{-1}). The results show that the electrochemical performance of Pt catalyst for ethanol oxidation is improved by the addition of PNR

Keywords Poly(neutral red) · Polymer · Platinum · Ethanol electrooxidation

1 Introduction

Direct ethanol fuel cells (DEFCs) have received great attention due to their high energy-conversion efficiency and low operating temperature. Among several alcohols which can be used in direct alcohol fuel cells (DAFCs), ethanol possesses distinct characteristics such as lower toxicity, low permeability across proton exchange membranes [1] and high energy density (8.01 kW h kg^{-1} for ethanol versus 6.09 kW h kg^{-1} for methanol) [2]. In particular, ethanol is a facile and abundant fuel which is easily produced in large quantities from agricultural products and through the fermentation of biomass.

Despite the merits of ethanol, the cleavage of the C–C bond is crucial and determines the fuel efficiency and electrical energy yield. Considerable efforts have been devoted towards the improvement of the activity and endurance of the anode electrocatalyst. These catalysts include Pt [3–5], Pt-based alloys [6–8] and oxide catalysts [9–13]. In addition, the choice of a suitable supporting material is also an important factor that may affect the performance of supported electrocatalysts owing to interactions between the electrocatalyst and the supporting material and surface reactivity [14]. Conductive polymers (such as polyaniline (PANI) [15, 16], polypyrrole (PPy) [17, 18], polythiophene (PTh) [19, 20], poly(*o*-phenylenediamine) (PoPD) [20], poly(N-acetylaniline) (PAANI) [21], poly(methylene blue) (PMB) [16]) have been shown to be suitable host matrices for dispersing metallic particles due to their very good conducting and mechanical properties and high stability [22]. Recently, neutral red (NR), an aniline derivative, containing a primary amino group, has received increasing attention. In particular, the electropolymerization of NR from both neutral [23–25] and acidic [23, 26, 27] aqueous solutions on various electrodes has been studied. Poly(neutral red) (PNR) possesses very good electrocatalytic activity toward the redox of small molecular compounds, e.g. electrooxidation of NO [28] and NADH [29, 30], and electroreduction of NO_2^-, IO_3^-, BrO_3^- [23] and NAD^+ [29].

X. Zhong · J. Chen (✉) · X. Zhang
State Key Laboratory of Chemo/Biosensing and Chemometrics,
College of Chemistry and Chemical Engineering, Hunan
University, Changsha 410082, People's Republic of China
e-mail: chenjinhua@hnu.cn

X. Zhong
College of Chemistry and Chemical Engineering, Guangxi
Normal University, Guilin 541004, People's Republic of China

Surprisingly, there are few investigations aimed at PNR as supports for electrocatalysts in DEFCs. From the foregoing viewpoint, this paper focuses mainly on the properties of PNR film as support for Pt particles in the electrocatalytic oxidation of ethanol. A PNR matrix was synthesized through electropolymerization. Pt particles were deposited on the PNR film by electrodeposition to obtain the Pt/PNR/graphite electrode; this showed much higher activity and stability for ethanol oxidation in acidic medium than Pt particles directly loaded on to a graphite electrode. PNR film may have potential application in DEFCs.

2 Experimental

2.1 Chemicals and instruments

A graphite substrate (6.0 mm in width, 11.8 mm in length, and 3.2 mm in height) was used as the working electrode. The apparent surface area of the working electrode was 0.71 cm^2. A standard three-electrode cell was employed with Pt wire as the counter electrode and a saturated calomel electrode (SCE) as the reference electrode. A CHI660A electrochemical workstation (CH Instruments, Inc) was employed for the electropolymerization of NR, the electrochemical deposition of Pt and electrochemical studies of these electrodes.

All chemicals were of analytical grade. All experiments were carried out at ambient temperature (298 K). All the potentials were referred to SCE. Freshly double-distilled water was used throughout.

The morphology and elemental composition of the Pt/PNR/graphite electrode were investigated by scanning electron microscopy (SEM, JSM 6700 F, operating at 20 kV), and energy dispersive X-ray spectroscopy (EDS, Vantage 4105, NORAN), respectively.

2.2 Preparation of the Pt/PNR/graphite electrode and electrochemical studies

Before the polymerization of NR, the graphite electrode was pretreated in 30 wt.% HNO_3 aqueous solution for 2 h to eliminate impurities at the surface and to activate the graphite substrate. To further increase the electrochemical activity, the electrode was cycled for 60 cycles in a 0.1 M H_2SO_4 aqueous solution in the potential range $-0.15 \sim 1.3$ V at a sweep rate of 50 mV s^{-1}. The PNR/graphite electrode was prepared from 5×10^{-4} M NR in a 0.5 M H_2SO_4 by typical cycle voltammetry (CV) in the potential range $-0.2 \sim 0.8$ V at a sweep rate of 50 mV s^{-1}. The PNR/graphite electrode was then rinsed with double-distilled water three times and Pt particles were electrodeposited on the surface of the PNR-modified graphite electrode by a potential-step deposition method from N_2 saturated 1.5 mM H_2PtCl_6 aqueous solution. The potential jumped from the open-circuit potential to -0.15 V (vs. SCE) with a pulse width of 0.001 s and the electrodeposition of Pt particles was carried out successively until a predetermined Pt deposition charge (Q_{dep}) was reached. After Pt deposition, the samples were washed in double-distilled water. To investigate the effect of the polymerization cycle number of NR on the electrocatalytic activity of the corresponding Pt/PNR/graphite electrodes for ethanol electrooxidation, a series of Pt/PNR/graphite electrodes, in which PNR was obtained with different polymerization cycle numbers, were prepared according to the process detailed above. In typical experiments, the polymerization cycle numbers were 5, 10, 15, 25, 150 cycles, and the corresponding Pt/PNR/graphite electrodes are labelled as Pt/PNR/graphite-1, Pt/PNR/graphite-2, Pt/PNR/graphite-3, Pt/PNR/graphite-4 and Pt/PNR/graphite-5, respectively.

Electrochemical properties of the Pt/PNR/graphite electrodes for ethanol electrooxidation were investigated in 1.0 M CH_3CH_2OH + 0.1 M H_2SO_4 aqueous solution by CV and chronoamperometry (CA). For comparison a Pt/graphite electrode without PNR was prepared according to the same procedure mentioned above and the corresponding electrochemical performance was also investigated.

3 Results and discussion

3.1 Electropolymerization of NR on the graphite electrode

The electrochemical polymerization of NR on the graphite electrode was performed by consecutive cyclic voltammetry from -0.2 to 0.8 V in 0.1 M H_2SO_4 solution containing 5×10^{-4} M NR. The cyclic voltammograms for the growth of PNR film are shown in Fig. 1, in which $i - E$ curves from the first to the tenth cycle were recorded. One redox couple, which corresponds to the NR redox reaction [23, 26, 27], can be observed at about -0.06 V. The current of the redox couple at about -0.06 V increases with increase in cycle number, indicating progressive growth of the PNR film.

3.2 The micrography and elemental composition of the Pt/PNR/graphite electrode

The morphology of the Pt particles dispersed on the PNR conducting polymer and the elemental composition of Pt/PNR/graphite electrode-2 were investigated by SEM and EDS. The results are shown in Figs. 2 and 3. Figure 2a shows that the graphite electrode is covered with PNR film.

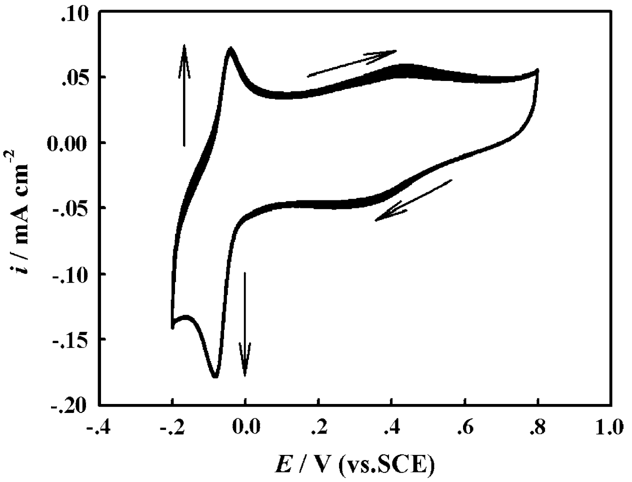

Fig. 1 Cyclic voltammograms for the electropolymerization of neutral red in 5×10^{-4} M NR + 0.5 M H_2SO_4 solution. Scan rate 50 mV s^{-1}

From Fig. 2b, most of Pt particles are seen to be electrodeposited on the PNR film and few Pt particles are observed on the graphite substrate. This indicates that PNR is suitable as the host material for Pt particles. For comparison, the SEM image of the Pt/graphite electrode with similar Pt deposition charge is shown in Fig. 2c. Pt particles are deposited homogeneously on the graphite substrate. Although the size of Pt/PNR particles is larger than that of Pt particles on the Pt/graphite electrode, the sizes of Pt particles on both Pt/PNR/graphite electrode and Pt/graphite electrode are similar. However, the electrocatalytic properties of Pt particles may be enhanced when "hard" interaction between Pt and graphite is changed to "soft" interaction between Pt and PNR. On the other hand, the EDS pattern of Pt/PNR/graphite electrode shown in Fig. 3 indicates that Pt and C are the major elements. The EDS result further confirms that Pt particles are successfully loaded onto the surface of the PNR/graphite electrode.

3.3 Electrocatalytic properties of the Pt/PNR/graphite electrode for ethanol oxidation

Electrochemical properties of the Pt/PNR/graphite electrode-2 were investigated by CV in 1.0 M CH_3CH_2OH + 0.1 M H_2SO_4 aqueous solutions. For comparison, electrochemical properties of graphite, PNR/graphite and Pt/graphite electrodes were also investigated under the same conditions. The corresponding cyclic voltammograms (CVs) are shown in Fig. 4. From Fig. 4a, a pair of redox peaks at about 0.3 ~ 0.4 V (vs. SCE) can be observed on both PNR/graphite and graphite electrodes. This may correlate with the redox behavior of the functional groups (such as –COOH, –OH) on carbon which are attributable to activation of the graphite electrode in acidic aqueous

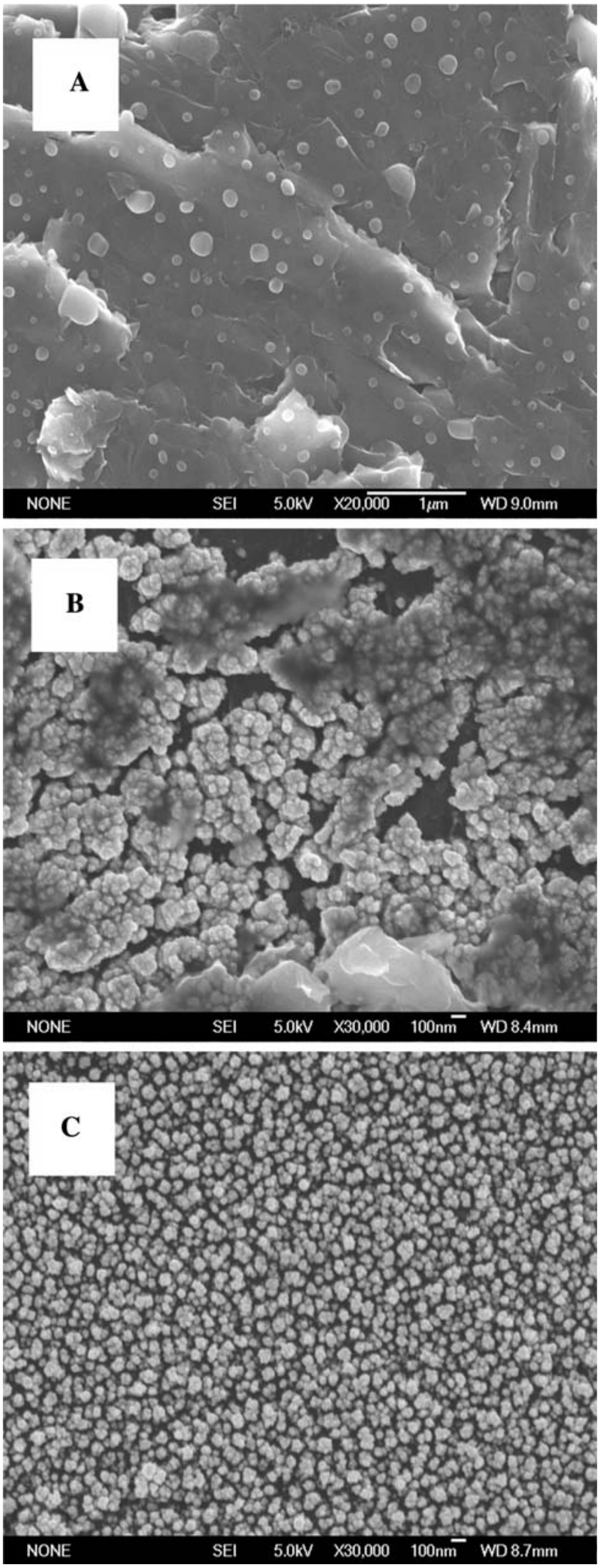

Fig. 2 SEM images of the PNR/graphite electrode (**a**), Pt/PNR/graphite electrode-2 (**b**) (Pt deposition charge, 4.71 μC cm^{-2}) and Pt/graphite electrode (**c**) (Pt deposition charge 4.36 μC cm^{-2})

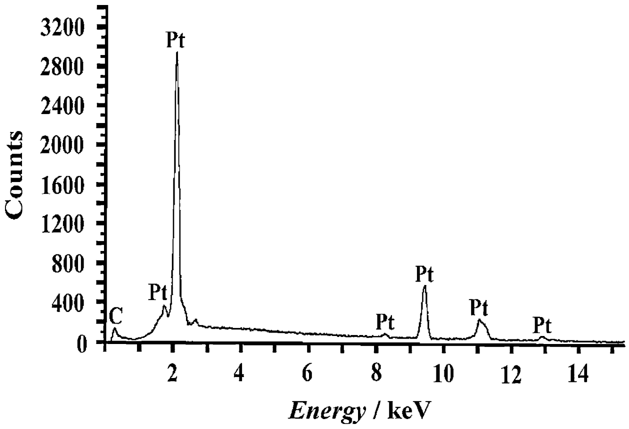

Fig. 3 EDS pattern of the Pt/PNR/graphite electrode-2 (Pt deposition charge 4.71 μC cm^{-2})

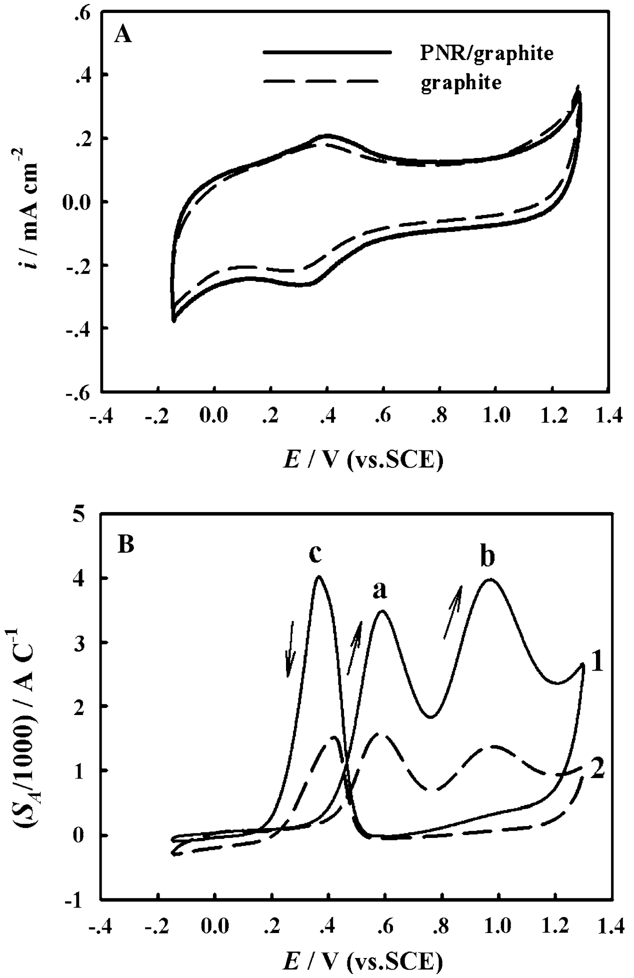

Fig. 4 Cyclic voltammograms of various electrodes at 50 mV s^{-1} in 1.0 M CH_3CH_2OH + 0.1 M H_2SO_4 aqueous solution. (**a**) PNR/graphite (curve 1) and graphite (curve 2) electrodes; (**b**) Pt/PNR/graphite electrode-2 (curve 1, Pt deposition charge, 4.71 μC cm^{-2}), Pt/graphite electrode (curve 2, Pt deposition charge 4.36 μC cm^{-2})

solution. The CV current density of the electrode increases in the presence of PNR. Also, no current peaks corresponding to ethanol oxidation can be seen in Fig. 4a, which indicates that both PNR and graphite substrate have no electrocatalytic activity for ethanol oxidation, whereas, the typical cyclic voltammograms of ethanol oxidation can be observed at both Pt/PNR/graphite electrode-2 and Pt/graphite electrode (curves 1 and 2 in Fig. 4b). Typical features of ethanol oxidation, agreeing with other work [30], are observed in Fig. 4b. Among these, two oxidation peaks are found at ~0.585 V and ~0.975 V (vs. SCE) during the forward scan. The first oxidation peak (peak a) corresponds mainly to the formation of CO_2, the second (peak b) corresponds mainly to the formation of CH_3COOH, and the third (peak c) in the reverse scan corresponds mainly to the formation of CH_3CHO [30, 31]. The onset potential for ethanol electrooxidation on Pt/PNR/graphite electrode-2 is lower than that on Pt/graphite. The addition of PNR leads to a negative shift of the onset potential for ethanol electrooxidation. On the other hand, the specific activity (S_A) defined by peak current density per unit of catalyst deposition charge is introduced and calculated by the following equation [32]:

$$S_A = 1000 i_{pa}/Q \tag{1}$$

where i_{pa} (mA cm^{-2}) is the peak current density obtained from the forward CV scan (peak a), and Q (μC cm^{-2}) is the deposition charge of Pt catalyst (it is assumed that the charge efficiency for Pt electrochemical deposition is the same (100%) on both the graphite and PNR/graphite electrodes.). According to Eq. 1, the S_A of the Pt/PNR/graphite electrode-2 at peak a can be calculated and is 3,478 A C^{-1}, which is about 2.20 times higher than that of the Pt/graphite electrode (1,582 A C^{-1}). Higher S_A values at peaks b and c are also observed at the Pt/PNR/graphite electrode-2. These imply that the electrocatalytic activities of the Pt/graphite electrode are enhanced by the introduction of PNR. This may be explained as follows: (1) the presence of PNR film is beneficial to the stabilization of the Pt nanocluster structures; (2) the donor-acceptor ability of PNR is favorable for accumulating and transferring oxygen-containing species (OH_{ads}) or H [21]. These species may react with CO-like intermediate species on the surface of Pt particles to release the active sites for further ethanol oxidation; (3) compared with the "hard" interaction between Pt and graphite in the Pt/graphite electrode, the "soft" interaction between Pt and PNR film may enhance the electrocatalytic properties of the Pt/PNR/graphite electrode. The exact reasons for the electrocatalytic activity of Pt enhanced by the PNR film are still not clear and require more experimental investigation.

Figure 5 shows the chronoamperograms (CAs) of the Pt/graphite electrode and the Pt/PNR/graphite electrode-2 at 0.5 V in 1.0 M CH_3CH_2OH + 0.1 M H_2SO_4 aqueous

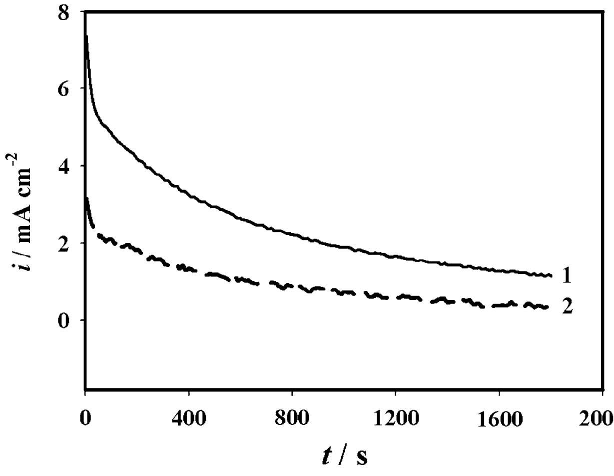

Fig. 5 Chronoamperograms of Pt/PNR/graphite electrode-2 (curve 1, Pt deposition charge 4.71 μC cm^{-2}) and Pt/graphite electrode (curve 2, Pt deposition charge, 4.36 μC cm^{-2}) at 0.5 V in 1.0 M CH_3CH_2OH + 0.1 M H_2SO_4 aqueous solution

solutions. When the potential is fixed at 0.5 V, a gradual decay of current density with time is observed on both the Pt/graphite electrode and the Pt/PNR/graphite electrode-2. As seen from Fig. 5, the current density of ethanol oxidation on the Pt/PNR/graphite electrode-2 decreases more slowly for the whole time (curve 1 in Fig. 5), compared with that on the Pt/graphite electrode (curve 2 in Fig. 5). After 1,800 s the current density remains 15.59 and 10.79% of the onset current density for the Pt/PNR/graphite electrode-2 and the Pt/graphite electrode, respectively. Moreover, the current density on the Pt/PNR/graphite electrode-2 (1.15 mA cm$^{-2)}$ is about 3.38 times higher than that on the Pt/graphite electrode (0.34 mA cm^{-2}). This implies further that the Pt/PNR/graphite electrode-2 exhibits higher electrocatalytic activity than the Pt/graphite electrode. The improved activity and better stability of the Pt/PNR/graphite electrode-2 may result from the assistance of PNR, which may reduce the accumulation of poisonous specious (such as CO_{ads}) on the surface of the Pt particles.

3.4 Effect of the polymerization cycle number of NR on ethanol electrooxidation

In order to investigate the effect of NR polymer thickness on ethanol oxidation, the relation of polymerization cycle number and S_A of peak a on different electrodes for ethanol electrooxidation was studied. The results are shown in Fig. 6. The S_A order of peak a on different Pt/PNR/graphite electrodes is as follows: Pt/PNR/graphite electrode-2 (3,478 A C^{-1}) > Pt/PNR/graphite electrode-1 (2,943 A C^{-1}) > Pt/PNR/graphite electrode-3 (2,915 A C^{-1}) > Pt/PNR/graphite electrode-4 (2,156 A C^{-1}) > Pt/PNR/graphite electrode-5 (1,591 A C^{-1}) > Pt/graphite (1,582 A C^{-1}). This means that the polymerization cycle number affects the S_A of peak a. In the range of investigation, the S_A of peak a for the Pt/PNR/graphite electrode increases with increase in polymerization cycle number and the maximum value is obtained at the tenth cycle. When the polymerization cycle number increases further the S_A of peak a decreases.

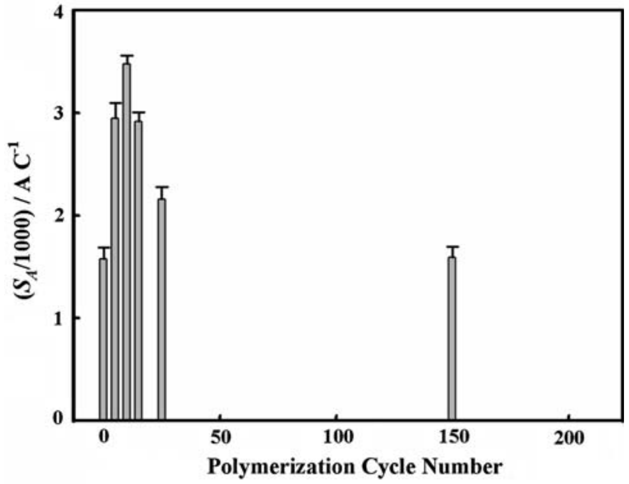

Fig. 6 Variation of the specific activity (S_A) of peak a of ethanol electrooxidation on different electrodes in 1.0 M CH_3CH_2OH + 0.1 M H_2SO_4 aqueous solution with polymerization cycle number of neutral red (NR). Scan rate 50 mV s^{-1}

3.5 Long-term cycle stability of the Pt/PNR/graphite electrode

After the CVs of the Pt/PNR/graphite electrode-2 investigated in 1.0 M CH_3CH_2OH + 0.1 M H_2SO_4 aqueous solution were stable, the long-term cycle stability of the Pt/PNR/graphite electrode-2 was investigated in the same solution by CV and the corresponding results are shown in Fig. 7. When the potential was cycled continuously for 250 cycles, 31% loss of peak current density obtained at the forward scan (i_{pa}) was observed for the Pt/PNR/graphite electrode-2 (curve 1). However, for the Pt/graphite electrode (curve 2), a larger decrease (49.81%) was observed. The reasons for the decay of i_p may be as follows: accumulation of poisonous specious (such as CO_{ads}) on the surface of the Pt particles, ethanol consumption during the successive scans and change in the surface structure of the Pt catalyst. The results from Fig.7 imply that the presence of PNR is helpful in improving the long-term cycle stability of Pt catalyst during ethanol electrooxidation. The increased stability was related to the reduction of the accumulation of poisonous species (such as CO_{ads}) on the surface of the Pt particles and stabilization of nanostructures by the PNR coating environment. The adsorption of CO on the PNR supported Pt surface may be less stable in comparison with that on bare Pt [21].

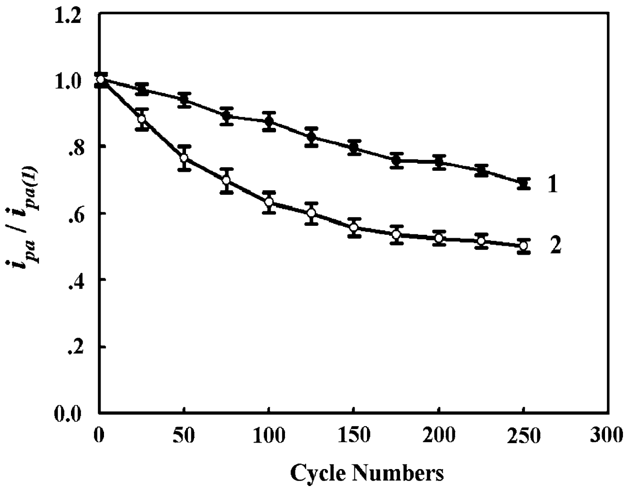

Fig. 7 Long-term cycle stability of the Pt/PNR/graphite electrode-2 (curve 1, Pt deposition charge 4.71 μC cm^{-2}) and Pt/graphite electrode (curve 2, Pt deposition charge 4.36 μC cm^{-2}) in 1.0 M CH_3CH_2OH + 0.1 M H_2SO_4 aqueous solution at 50 mV s^{-1}. i_{pa}, the peak current density of peak a; $i_{pa\ (1)}$, the peak current density of peak a at the first cycle

After 250 cycles, the electrode was stored in double-distilled water for 24 h, and the CV experiments were carried out again in fresh ethanol solution. The peak current density of the Pt/PNR/graphite electrode-2 still retains 88.56% of the value of the $i_{pa(1)}$ (the peak current density for peak a at the first cycle). Whereas, for the Pt/graphite electrode, only 63.31% of the value of $i_{pa(1)}$ was retained. This further confirms that the Pt/PNR/graphite electrode has better long-term stability and storage properties than the Pt/graphite electrode, thus indicating that PNR is a promising matrix for dispersing metallic particles.

4 Conclusions

PNR/graphite as a support material for Pt was prepared and used for ethanol electrooxidation in acidic medium. The electrocatalytic activity of the resulting electrode, namely the Pt/PNR/graphite electrode, was investigated by electrochemical methods. The specific activity (S_A) at peak a of the Pt/PNR/graphite electrode-2 in which NR was polymerized for 10 cycles in 5 × 10^{-4} M NR + 0.5 M H_2SO_4 solution was 3,478 A C^{-1} and about 2.20 times higher than that of Pt/graphite electrode (1,582 A C^{-1}). Good electrochemical performance (higher electrocatalytic activity, good long-term cycle stability) of Pt loaded on the surface of the PNR/graphite electrode is attributable to the fact that the PNR provides a favourable environment for stabilizing the Pt and extracting intermediates and poisoning species.

Acknowledgments This work was supported by the Program for New Century Excellent Talents in University (NCET-04-0765), the Natural Science Foundation of China (50172014), and the Scientific Research Foundation for Returned Overseas Chinese Scholars, State Education Ministry (2001-498).

References

1. Fujiwara N, Friedrich KA, Stimming U (1999) J Electroanal Chem 472(2):120
2. Zhou WJ, Song SQ, Li WZ, Sun GQ, Xin Q, Kontou S, Poulianitis K, Tsiakaras P (2004) Solid State Ionics 175:797
3. Tang H, Chen JH, Nie LH, Liu DY, Deng W, Kuang YF, Yao SZ (2004) J Colloid Interface Sci 269(1):26
4. He ZB, Chen JH, Liu DY, Tang H, Deng W, Kuang YF (2004) Mater Chem Phys 85(2–3):396
5. Rajesh B, Karthik V, Karthikeyan S, Thampi KR, Bonard JM, Viswanathan B (2002) Fuel 81:2177
6. Neto AO, Giz MJ, Perez J, Ticianelli EA, Gonzalez ER (2002) J Electrochem Soc 149(3):A272
7. Leger JM, Rousseau S, Coutanceau C, Hahn F, Lamy C (2005) Electrochim Acta 50:5118
8. Tanaka S, Umeda M, Ojima H, Usui Y, Kimura O, Uchida I (2005) J Power Sources 152:34
9. Liu B, Chen JH, Zhong XX, Cui KZ, Zhou HH, Kuang YF (2007) J Colloid Interface Sci 307:139
10. Xu CW, Zeng R, Shen PK, Wei ZD (2005) Electrochim Acta 51:1031
11. Xu CW, Shen PK (2005) J Power Sources 142:27
12. Xu CW, Shen PK, Ji XH, Zeng R, Liu YL (2005) Electrochem Commun 7:1305
13. Bürgi T (2005) J Catal 229:55
14. Hu ZA, Ren LJ, Feng XJ, Wang YP, Yang YY, Shi J, Mo LP, Lei ZQ (2007) Electrochem Commun 9:97
15. Wu G, Li L, Li JH, Xu BQ (2005) Carbon 43:2579
16. Li X, Zhong M, Sun C, Luo YM (2005) Mater Lett 59:3913
17. Becerik I, Suzer S, Kadirgan F (1999) J Electroanal Chem 476:171
18. Moravcova S, Bouzek K (2005) J Electrochem Soc 152:A2080
19. Biallozor S, Kupniewska A (2004) Bull Electrochem 20:241
20. Golabi SM, Nozad A (2002) J Electroanal Chem 521:161
21. Jiang C, Lin X (2007) J Power Sources 164:49
22. Inzelt G, Pineri M, Schultze JW, Vorotyntsev MA (2000) Electrochim Acta 45(15–16):2403
23. Chen S-M, Lin K-C (2001) J Electroanal Chem 511:101
24. Karyakin AA, Ivanova YN, Karyakina EE (2003) Electrochem Commun 5:677
25. Benito D, Gabrielli C, García-Jareño JJ, Keddam M, Perrot H, Vicente F (2003) Electrochim Acta 48:4039
26. Broncová G, Shishkanova TV, Matějka P, Volf R, Král V (2004) Anal Chim Acta 511:197
27. Chen CX, Gao YH (2007) Electrochim Acta 52:3143
28. Tang XR, Fang C, Yao B, Zhang WM (1999) Microchem J 62:377
29. Karyakin AA, Bobrova OA, Karyakina EE (1995) J Electroanal Chem 399:179
30. Lamy C, Belgsir EM, Léger JM (2001) J Appl Electrochem 31:799
31. Pacheco Santos V, Del Colle V, Batista de Lima R, Tremiliosi-Filho G (2007) Electrochim Acta 52:2376
32. Zhong XX, Chen JH, Liu B, Xu Y, Kuang YF (2007) J Solid State Electrochem 11:463